

Network-Enhanced Photoresponse Time of Ge Nanowire Photodetectors

Chaoyi Yan, Nandan Singh, Hui Cai, Chee Lip Gan, and Pooi See Lee*

School of Materials Science and Engineering, Nanyang Technological University, Singapore 639798

ABSTRACT We demonstrated that the photoresponse time of Ge nanowire (NW) photodetectors could be greatly improved by using percolated NW networks (instead of single NW) as the active detection channels. Although the reset time for single-NW devices was >70 s, a fast reset time <1 s was observed for NW-network devices. The enhancement was attributed to the barrier-dominated conductance for network devices, which was not available in single-NW devices. The network structures provide ideal alternative solutions to the conventional single-NW photodetectors, given their superior performances and low-cost fabrication processes.

KEYWORDS: germanium nanowire • network • photoresponse time • photodetector • sensor

1. INTRODUCTION

Semiconducting one-dimensional (1D) nanomaterials have been widely used for chemical (1), biological (2) and light sensors (3). The nanostructures are expected to exhibit better performances (such as high sensitivity, high selectivity, fast response and reset time, etc.) than their bulk or thin film counterparts because of the high surface-to-volume ratio. Photodetection is one of the most important applications of nanowire (NW) sensors and extensive studies have been reported in literature (3–7). However, it should be highlighted that most of the previous studies focused on the photodetection using single-NW devices, which required complex, low-yield, and high-cost lithography techniques. Moreover, the difficulty in NW assembly has seriously hindered the development of large scale single-NW devices. Alternatively, macroscale NW-network devices have been of increasing interest recently because they exhibit sufficiently good or even better performances but require only facile and low-cost fabrication techniques (8–10). Despite the fact that NW-network devices allow potential large scale fabrication, investigations of their photodetection performances and advantages are quite limited until now.

Ge ($E_g = 0.68$ eV) has been considered as a promising material for photodetection because it responds to a wide spectral range (from ultraviolet to infrared) and is compatible with Si technology (11, 12). Previously, GeNW arrays embedded in anodized aluminium oxide (AAO) template (5) and single GeNW field effect transistors (FETs) (13) have been used for visible-light detection. However, no efforts have been devoted to improve the photoresponse time of GeNW photodetectors. Fast response and reset time is one of the highly desirable characteristics for industrial photodetection applications (7) but has attracted less focus than the studies of, for example, sensing mechanisms and sensitivity improvement (4, 14). In this report, we demonstrate that the

photoresponse time of GeNW photodetectors can be significantly improved by using percolated GeNW networks, instead of single NW, as building blocks. The enhancement was attributed to the unique barrier dominated conduction mechanism for NW networks. The NW-network devices with low-cost fabrication and superior performances provide promising alternative solutions than the single-NW structure for future photodetectors.

2. EXPERIMENTAL METHODS

The GeNWs were synthesized in a horizontal double-tube system as reported earlier (15, 16). Mixed Ge and carbon powder (~ 0.5 g, weight ratio 1:1) was placed at the sealed end of a small quartz tube. Cleaned Si (100) substrates pre-coated with 9 nm Au film were placed at the open end of the small quartz tube for product collection. Then the small quartz tube was loaded into the furnace chamber, with sealed end at the central high temperature region. The temperature of the furnace was increased to 1000 °C at a rate of 15 °C min^{-1} and kept for 60 min under a constant Ar flow of 200 sccm (standard cubic centimeter per minute). The temperature of the Si substrates during growth was in the range of 300–400 °C. The furnace was allowed to cool naturally to room temperature after growth. Morphologies and structures of the products were characterized using scanning electron microscopy (SEM, JEOL 6340F), transmission electron microscopy (TEM, JEOL 2010), and energy-dispersive spectroscopy (EDS). For TEM and EDS analyses, the NWs were dispersed in ethanol by ultra-sonication for 1 min, and the solutions were then dropped on a Cu grid coated with holey carbon film. The samples were dried naturally in air before analysis.

For device fabrication, standard optical-lithography followed by Cr/Au (10/50 nm) deposition and liftoff was used to define the contact electrodes. GeNWs suspended in ethanol were dispersed on top of the electrodes. The NW concentration in solution was adjusted to obtain single-NW and NW-network devices. The contact conditions of single-NW devices were improved by Pt deposition in FIB system.

* Corresponding author. E-mail: pslee@ntu.edu.sg.

Received for review April 12, 2010 and accepted June 18, 2010

DOI: 10.1021/am100321r

2010 American Chemical Society

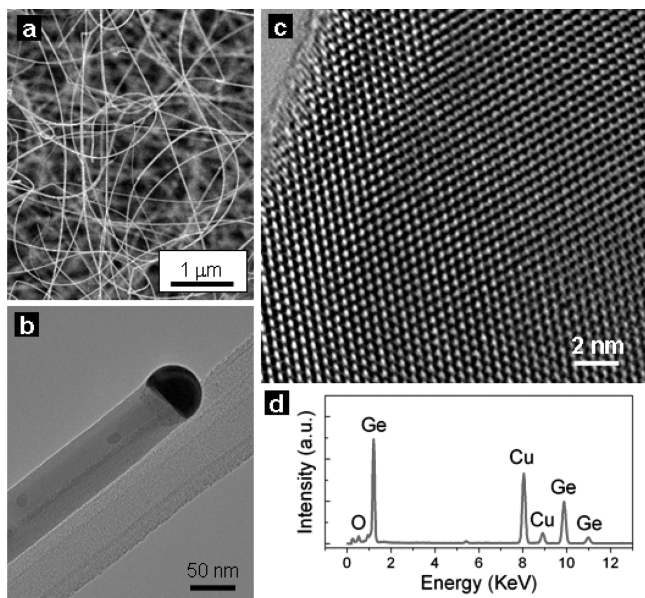


FIGURE 1. (a) SEM, (b) TEM, (c) HRTEM, and (d) EDS results of the single-crystalline GeNWs grown via Au-catalyzed VLS method.

Photoresponse characteristics of the GeNW photodetectors were measured in Keithley semiconductor parameter analyzer. Tungsten-halogen lamp with tunable light intensity in the probe station was used as light source. Typical wavelength spectra of the light source are shown in Figure S1 in the Supporting Information. All the measurements were performed at room temperature in ambient conditions.

3. RESULTS AND DISCUSSION

Morphologies and structures of the as-synthesized GeNWs are shown in Figure 1. A typical low-magnification SEM image of the GeNWs is shown in Figure 1a. Diameters of the NWs are in the range of 10–80 nm, with lengths of tens of micrometers. The GeNWs were grown via Au-catalyzed vapor-liquid-solid (VLS) mechanism (17), as verified by the Au nanoparticles at NW growth front (Figure 1b). Lattice-resolved high-resolution TEM (HRTEM) image of the GeNW is depicted in Figure 1c, showing the single-crystalline nature of the NWs. Chemical compositions of the NWs were analyzed by EDS equipment attached in the TEM system, and the spectrum (Figure 1d) reveals that the NWs are composed of Ge. The small O peak may originate from the thin surface oxide layer, and Cu peaks are from the Cu grid used for TEM characterizations.

Visible-light photodetectors based on single NW and NW networks were fabricated for comparison studies. Schematic model, I – V curve, and photoresponse characteristic of the single-NW devices are shown in Figure 2a–c, respectively. Diluted NW solution was used to reduce the NW concentration and facilitate single-NW device fabrication. Focused-ion-beam (FIB) deposited Pt pads were used to obtain reliable contacts between the NW and underlying Au electrodes. A representative SEM image of the single-NW device is shown in Figure 2b inset. Ohmic conductance was observed for those single-NW devices, as suggested by the highly linear I – V characteristic curves (Figure 2b). When the light was turned on ($\sim 0.8 \text{ mW cm}^{-2}$), the conductance increases from

1.41 to 1.44 nS at a fixed bias of 1 V. To further characterize the photoresponse behavior of the single-NW device, we measured current as a function of time when the light was turned on ($\sim 0.4 \text{ mW cm}^{-2}$) and off, as shown in Figure 2c. Slow response and reset time was observed. For example, the measured photocurrent reset time is larger than 70 s for the single-NW device (Figure 2c). Slow response and reset times of tens of seconds were typically observed for all the single-NW devices.

However, the response and reset time can be greatly improved by using NW networks (instead of single NW) as the active detection channel. Photoresponse performances of the network devices are shown in Figure 2e–f. Nonlinear I – V curves were typically observed for the network devices (Figure 2e), indicating a barrier-dominated conducting mechanism (details will be discussed below). The current as a function of time was measured to characterize the response and reset time for the network device, when the light was periodically turned on and off. A fully reversible switching behavior was observed. More importantly, the network devices exhibited fast response and reset time within 1 s. An enlarged view of the current decay process with a reset time of 0.2 s is shown in Figure 3a.

Fast photoresponse time is a highly desirable characteristic for commercial light sensing applications. It enriches the potential functionalities of photodetectors, such as the efficient tracing of light with variational intensities. As a typical example, the multi-step light detection using NW-network device was demonstrated (Figure 3b). The light intensities for the 3 steps are ~ 0.02 , 0.3, and 0.8 mW cm^{-2} , corresponding to the current levels of 0.1, 0.3, and $0.7 \mu\text{A}$, respectively. As can be clearly viewed, the fast response and reset time of the network devices enables the efficient depiction of the light intensity variations. However, the significant delay resulted from the slow response and reset time for the single-NW device makes them inferior choices. Note that the relative yield of single-NW and NW-network devices can be controlled by tuning the NW concentration in solution and the solution volume dropped between the electrodes. For our network devices, the NW densities were estimated to be typically in the range of 100–500. Although the current values of the network devices varied from device to device due to the different NW densities and contact conditions (conduction mechanisms will be discussed below), fast photoresponse time was exclusively observed for all the network devices (see Figure S2 in the Supporting Information), indicating a good reproducibility.

First we discuss the electron conduction mechanisms for the GeNW photodetectors. Schematic band diagrams of the single-NW and NW-network devices are shown in Figure 3c,d, respectively. It is known that GeNWs without surface passivation quickly form a thin oxide layer at the surface (18, 19). The high density of Ge/GeO_x interfacial states (negative charge traps) would induce hole accumulation at the NW surface, resulting in p -type semiconducting behavior for the namely undoped GeNWs (20, 21). It has also been experimentally demonstrated that the Fermi level at metal/

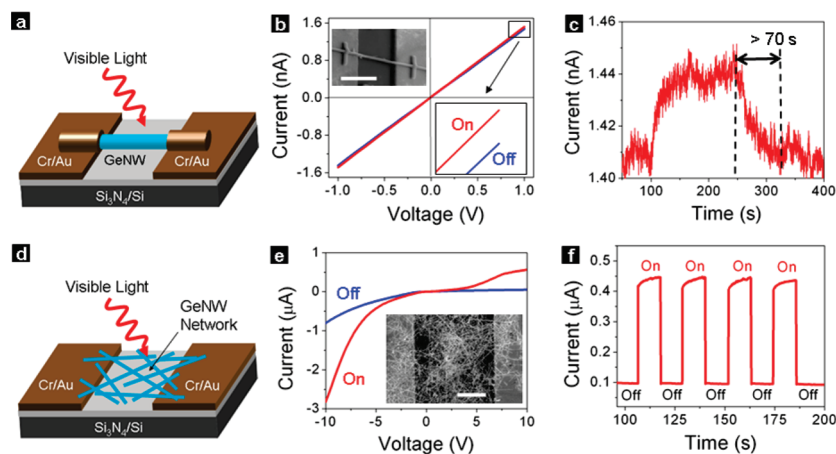


FIGURE 2. Comparison of the photoresponse behaviors of single-NW device and network device. Schematic models, I - V curves and photoresponse characteristics of (a–c) single-NW device and (d–f) NW-network device. The scale bars in the insets of b and e are 5 μm .

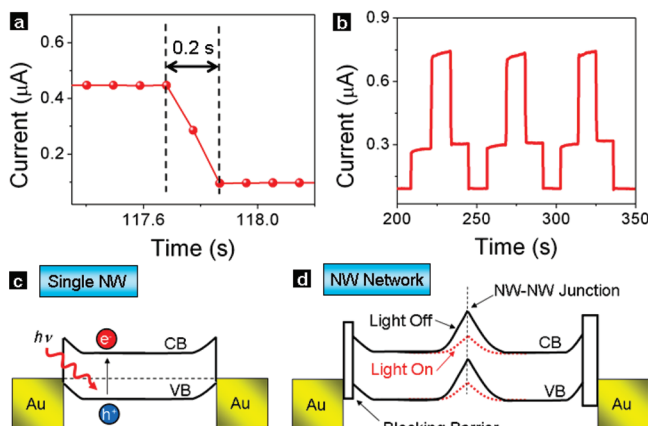


FIGURE 3. (a) Enlarged view of a current decay process showing the fast reset time of 0.2 s. (b) Multiple-step photoresponse characteristics of network devices. (c, d) Schematic band diagrams for single-NW device with Ohmic contact and network device with non-Ohmic contact, at zero bias. Rectangles in (d) represent the partial contributions that are not light-sensitive (see text for more details).

Ge interface is strongly pinned near the valence band edge of Ge (22), as shown in Figure 3c,d. As a result, the Schottky barrier at Au-GeNW interface is expected to be negligible considering the p -type conduction and Fermi level pinning (FLP) effect. This is consistent with the Ohmic conductance observed for single-NW devices (Figure 2b). It should be noted that the FIB-improved good contact conditions also contribute to the Ohmic conductance, by reducing the blocking barriers at the contact regions (see Figure 3d and discussion below).

Non-Ohmic and asymmetric conductance was observed for NW-network devices (Figure 2c), and can be understood based on the following aspects. First, significant blocking barriers exist at the Au-GeNW interfaces (Figure 3d), because of the poor contact conditions of the drop-cast process without further improvement (such as Pt deposition by FIB). The two blocking barriers possess different heights or widths, probably due to the different NW numbers and contact conditions. This explains why asymmetric conductance was observed for network devices (Figure 2e). The Au-GeNW blocking barrier (as well as the NW–NW junction barrier shown below) may physically originate from the small

contact area, thin surface insulating layer and surface adsorbates. Note that this blocking barrier can be effectively reduced during FIB etching/deposition processes, by enlarging the contact area, removing the surface insulating layer and adsorbates (see Figure S3 in the Supporting Information). Thus, good Ohmic contact was observed for the single-NW devices (Figure 2b). Second, the electron conduction in percolated NW networks is dominated by the NW–NW junction barriers (as indicated in Figure 3d) (10, 23, 24), which are not readily available in single-NW devices. Previous studies of individual NW–NW junction also revealed the dominant resistance of the junction barrier (25, 26). Both the blocking barrier at the Au-GeNW interface and NW–NW junction barrier contribute to the non-Ohmic conductance of the network devices. In Figure 3d, the rectangles (with different widths and heights) are used to represent the partial contributions from the small contact area and surface insulating layer, which are not light-sensitive. The rectangles are omitted in the NW–NW junction barrier for clarity purpose. The bending bands are used to represent the electron depletion/hole accumulation layers (response to incident light), which originate from the surface charge/adsorbates.

The different conduction mechanisms for the single-NW and NW-network devices lead to the distinct photoresponse behaviors. It is known that for GeNWs exposed in air, oxygen molecules would adsorb on the NW surface by capturing free electrons [$\text{O}_2(\text{g}) + \text{e}^- \rightarrow \text{O}_2^-(\text{ad})$] (4, 13). Both the charge traps and oxygen adsorbates contribute to the surface electron depletion and hole accumulation. Upon light illumination, electron-hole pairs can be generated [$h \rightarrow \text{e}^- + \text{h}^+$]. The holes (dominant carriers for p -type NW) would be attracted to the NW surface to fill the charge traps (discharging process) or desorb the oxygen adsorbates. The carrier densities would gradually increase as the traps are filled and the oxygen adsorbates are desorbed. It should be noted that both the hole diffusion (to discharge the negative charge traps) (20) and oxygen desorption processes (4) are quite slow, as have already been demonstrated in previous studies. Consequently, the carrier density (and hence conductivity) of the GeNW would increase gradually upon light illumination. For single-NW device with Ohmic contact, the

resistance is determined by the NW itself. The slow increase of the NW conductivity resulted in the slow response time (Figure 2c). An analogous current decaying process can be observed when the light was turned off. The slow surface trap charging and oxygen readsorption processes (reverse processes) lead to the slow photocurrent reset time, which was shown to be >70 s (Figure 2c).

The fast response and reset time for NW-network devices can be attributed to the barrier dominated conductance. Note that the surface charge and adsorbates induced band-bending (Figure 3d) are sensitive to incident light and can be treated as Schottky barriers (10). The NW–NW junction barrier is analogous to two back-to-back Schottky barriers. The increased carrier density (upon illumination) in GeNW would narrow the barrier width, which is equivalent to a lowering of the effective barrier height. As a result, the conductivity of the percolated NW network would increase, since the narrowed (lowered) barriers allow easier electron tunneling and transportation. It should be highlighted that this light-induced barrier height modulation is much faster than the trap discharging or oxygen diffusion processes (which usually accounts for photodetectors with Ohmic contact). For example, previous studies showed that the photocurrent response time for Au–CdS (27) and Pt–ZnO (7) Schottky barriers were typically below 1 s. However, the time required for trap discharging or oxygen diffusion was usually on the order of several minutes or up to hours (4, 14, 20, 28–30). Previously, Zhou et al. reported that the reset time of ZnO NW photodetectors could be enhanced by intentionally deposited Schottky contact on single NW (7). Here we show that the NW network devices with Schottky-like barrier-dominated conductance exhibited comparable performances. More importantly, network devices require less-intense lithography techniques and allow potential large-scale fabrications.

As discussed above, the fast photoresponse time is associated with the intrinsic property of the NW–NW junctions, which dominate the electron conduction in entangled NW networks. Recently, photodetectors using multiple ZnS nanobelts were demonstrated (31). Most of the ZnS nanobelts were in direct contact with the counter electrodes (quasi-parallel), and no photoresponse time enhancement was observed when compared with single ZnS nanobelt devices (31). The parallel NW device (positioned side-by-side, see Figure S4 in the Supporting Information) can be treated as multiple single-NW devices working simultaneously and independently. They should exhibit the same photoresponse time as single-NW device, although the current values would be enlarged correspondingly.

4. CONCLUSIONS

In conclusion, we have demonstrated that the response and reset time of GeNW photodetectors can be improved by using percolated NW networks as active channel material. While single-NW devices with Ohmic contact showed slow reset time over 70 s, NW-network devices with non-Ohmic contact showed much faster current reset time within 1 s. The enhanced performances of network devices were attributed to the unique NW–NW junction barrier dominated

conductance. Those intrinsic junction barriers exhibited Schottky-barrier like fast modulation rates upon light illumination. The superior performances associated with NW networks, together with their facile and cost-effective fabrication processes, are expected to greatly expand their potential applications in photodetectors.

Acknowledgment. The authors gratefully acknowledge X. W. Lu, M. F. Lin, S. C. Lim, and J. Guo for their insightful discussions and technical support.

Supporting Information Available: Additional materials (PDF). This material is available free of charge via the Internet at <http://pubs.acs.org>.

REFERENCES AND NOTES

- (1) McAlpine, M. C.; Ahmad, H.; Wang, D. W.; Heath, J. R. *Nat. Mater.* **2007**, *6*, 379.
- (2) Zheng, G. F.; Patolsky, F.; Cui, Y.; Wang, W. U.; Lieber, C. M. *Nat. Biotechnol.* **2005**, *23*, 1294.
- (3) Kind, H.; Yan, H. Q.; Messer, B.; Law, M.; Yang, P. D. *Adv. Mater.* **2002**, *14*, 158.
- (4) Soci, C.; Zhang, A.; Xiang, B.; Dayeh, S. A.; Aplin, D. P. R.; Park, J.; Bao, X. Y.; Lo, Y. H.; Wang, D. *Nano Lett.* **2007**, *7*, 1005.
- (5) Polyakov, B.; Daly, B.; Prikulis, J.; Lisauskas, V.; Vengalis, B.; Morris, M. A.; Holmes, J. D.; Erts, D. *Adv. Mater.* **2006**, *18*, 1812.
- (6) Hsieh, C. H.; Chou, L. J.; Lin, G. R.; Bando, Y.; Golberg, D. *Nano Lett.* **2008**, *8*, 3081.
- (7) Zhou, J.; Gu, Y. D.; Hu, Y. F.; Mai, W. J.; Yeh, P. H.; Bao, G.; Sood, A. K.; Polla, D. L.; Wang, Z. L. *Appl. Phys. Lett.* **2009**, *94*, 191103.
- (8) Unalan, H. E.; Zhang, Y.; Hiratal, P.; Dalal, S.; Chu, D. P.; Eda, G.; Teo, K. B. K.; Chhowalla, M.; Milne, W. I.; Amaratunga, G. A. J. *Appl. Phys. Lett.* **2009**, *94*, 163501.
- (9) Cao, Q.; Kim, H. S.; Pimparkar, N.; Kulkarni, J. P.; Wang, C. J.; Shim, M.; Roy, K.; Alam, M. A.; Rogers, J. A. *Nature* **2008**, *454*, 495.
- (10) Yan, C. Y.; Singh, N.; Lee, P. S. *Appl. Phys. Lett.* **2010**, *96*, 053108.
- (11) Tang, L.; Kocabas, S. E.; Latif, S.; Okyay, A. K.; Ly-Gagnon, D. S.; Saraswat, K. C.; Miller, D. A. B. *Nat. Photonics* **2008**, *2*, 226.
- (12) Assefa, S.; Xia, F. N.; Vlasov, Y. A. *Nature* **2010**, *464*, 80.
- (13) Ahn, Y. H.; Park, J. *Appl. Phys. Lett.* **2007**, *91*, 162102.
- (14) Lao, C. S.; Park, M. C.; Kuang, Q.; Deng, Y. L.; Sood, A. K.; Polla, D. L.; Wang, Z. L. *J. Am. Chem. Soc.* **2007**, *129*, 12096.
- (15) Yan, C. Y.; Lee, P. S. *J. Phys. Chem. C* **2009**, *113*, 14135.
- (16) Yan, C. Y.; Chan, M. Y.; Zhang, T.; Lee, P. S. *J. Phys. Chem. C* **2009**, *113*, 1705.
- (17) Wanger, R. S.; Ellis, W. C. *Appl. Phys. Lett.* **1964**, *4*, 89.
- (18) Zhang, L.; Tu, R.; Dai, H. J. *Nano Lett.* **2006**, *6*, 2785.
- (19) Wang, D. W.; Chang, Y. L.; Wang, Q.; Cao, J.; Farmer, D. B.; Gordon, R. G.; Dai, H. J. *J. Am. Chem. Soc.* **2004**, *126*, 11602.
- (20) Hanrath, T.; Korgel, B. A. *J. Phys. Chem. B* **2005**, *109*, 5518.
- (21) Sdong, H. K.; Jeon, E. K.; Kim, M. H.; Oh, H.; Lee, J. O.; Kim, J. J.; Choi, H. J. *Nano Lett.* **2008**, *8*, 3656.
- (22) Nishimura, T.; Kita, K.; Toriumi, A. *Appl. Phys. Lett.* **2007**, *91*, 123123.
- (23) Sysoev, V. V.; Goschnick, J.; Schneider, T.; Strelcov, E.; Kolmakov, A. *Nano Lett.* **2007**, *7*, 3182.
- (24) Kolmakov, A.; Potluri, S.; Barinov, A.; Montes, T. O.; Gregoratti, L.; Nino, M. A.; Locatelli, A.; Kiskinova, M. *ACS Nano* **2008**, *2*, 1993.
- (25) Cui, Y.; Lieber, C. M. *Science* **2001**, *291*, 851.
- (26) Duan, X. F.; Huang, Y.; Cui, Y.; Wang, J. F.; Lieber, C. M. *Nature* **2001**, *409*, 66.
- (27) Lubberts, G.; Burkey, B. C.; Bucher, H. K.; Wolf, E. L. *J. Appl. Phys.* **1974**, *45*, 2180.
- (28) Liu, Y.; Zhang, Z. Y.; Xu, H. L.; Zhang, L. H.; Wang, Z. X.; Li, W. L.; Ding, L.; Hu, Y. F.; Gao, M.; Li, Q.; Peng, L. M. *J. Phys. Chem. C* **2009**, *113*, 16796.
- (29) He, J. H.; Chang, P. H.; Chen, C. Y.; Tsai, K. T. *Nanotechnology* **2009**, *20*, 135701.
- (30) Fang, F.; Futter, J.; Markwitz, A.; Kennedy, J. *Nanotechnology* **2009**, *20*, 245502.
- (31) Fang, X. S.; Bando, Y.; Liao, M. Y.; Zhai, T. Y.; Gautam, U. K.; Li, L.; Koide, Y.; Golberg, D. *Adv. Funct. Mater.* **2010**, *20*, 500.

AM100521R